EUROPEAN FUSION DEVELOPMENT AGREEMENT

JET

EFDA–JET–PR(04)01

D.J. Kelliher, N.C. Hawkes, P.J. McCarthy, and JET EFDA contributors

Comparison of TRANSP-Evolved q-Profiles with MSE Constrained Equilibrium Fits on JET

Comparison of TRANSP-Evolved q-Profiles with MSE Constrained Equilibrium Fits on JET

D.J. Kelliher[1], N.C. Hawkes[2], P.J. McCarthy[3],
and JET EFDA contributors*

[1]Department of Physics, University College Cork, Association EURATOM-DCU, Cork, Ireland
[2]EURATOM/UKAEA Fusion Association, Culham Science Centre, Abingdon, Oxon. OX14 3DB, UK
[3]Institut für Plasmaphysik, Forschungszentrum Jülich GmbH, EURATOM Association,
Trilateral Euregio Cluster, D- 52425 Jülich, Germany
** See annex of J. Pamela et al, "Overview of Recent JET Results and Future Perspectives",*
Fusion Energy 2000 (Proc. 18th Int. Conf. Sorrento, 2000), IAEA, Vienna (2001).

Preprint of Paper to be submitted for publication in
Plasma Physics and Controlled Fusion

ABSTRACT.
The pitch angle predicted by the transport analysis code TRANSP was compared with Motional Stark effect (MSE) data. TRANSP was initialised in early rampup phase using a measured pitch angle profile but evolved the current profile using the magnetic field diffusion equation thereafter. The comparison was carried out on a wide range of pulses, including cases where a current hole was established in the preheating phase. Beyond confirming that a neoclassical model of the resistivity is superior to the classical one in modelling the evolution of the current profile in JET, the results indicate that the TRANSP prediction is nearly always within the 95% confidence band of the MSE data. In addition, it is shown that the TRANSP q-profile is consistent with MHD data and Faraday rotation polarimetry data.

1. INTRODUCTION

The ability to model the current diffusion in tokamak plasmas using codes such as TRANSP [1] is predicated on knowing the resistivity as well as the accurate modelling of non-inductive current drive. As well as the classical model due to Spitzer [2], a series of neoclassical models take into account the trapped particle fraction present in axisymmetric toroidal systems. This paper is concerned *inter alia* with testing the validity of the classical and various neoclassical models on JET.

Studies on other tokamaks have confirmed that in large devices trapped particles must be taken into account [3]–[7]. The prediction of integrated quantities such as the loop voltage or mean Z-effective have been adopted as resistivity model tests at TFTR [3] and JET [9] respectively. Other studies have inferred that the resistivity is neoclassical at JET [10], [11]. A more thorough test is afforded by a direct comparison of the TRANSP magnetic pitch angle profile with Motional Stark Effect (MSE) measurements. Such a comparison has already found in favour of a neoclassical model of resistivity at TFTR [6] and DIII-D [12].

Further to confirming that a neoclassical model better describes the evolution of the plasma current profile at JET, it is desirable that an estimate of its accuracy be obtained. An accurate model of the resistivity would allow the inductive current to be calculated with confidence. Furthermore, a reliable bootstrap model and beam-driven current calculation would allow the total current profile to be evolved. A comprehensive Monte Carlo calculation ensures that the beam-driven current is accurately found [8]. Used as an internal constraint in a magnetic equilibrium code, MSE pitch angle data allows the q-profile to be accurately reconstructed [13]. This safety factor profile (q-profile) can be compared with that obtained via current diffusion. The practical goal is that the current profile , with a known initial state e.g. from standard, reproducible current ramp-up scenarios, could be found with an acceptable accuracy even during times when MSE data is unavailable.

In this paper, we will compare the pitch angle profile measured by the MSE diagnostic with that predicted by the time dependent transport code TRANSP when using either Spitzer or various models of neoclassical resistivity and bootstrap current combined with other non-inductive contributions. Since the bootstrap current is a consequence of the trapped particles (and so is a neoclassical effect), it is not included when using Spitzer resistivity in the code.

The accuracy of the neoclassical predictions is determined by calculating the root mean squared error of the TRANSP prediction. In addition to constraints provided by the MSE data, the TRANSP prediction is, where possible, checked for consistency against MHD events and Faraday rotation data. The analysis was carried out on a wide variety of discharge types, including cases where current holes exist [14], so that the conditions under which the neoclassical model best predicts the pitch angle may be ascertained. The range of discharges studied for the purposes of this investigation was limited to those without LHCD during the main heating phase (discharges with LHCD in the pre-heating phase were included).

2. ANALYSIS METHODOLOGY

The time dependent code TRANSP [1] in its 'primary' mode, uses the magnetic field diffusion equation

$$\frac{\partial \boldsymbol{B}}{\partial t} = \frac{\eta}{\mu} \nabla^2 \mathbf{B} - \nabla \frac{}{} \times (\nabla \times \mathbf{B}) + \nabla \times (\eta J_{NI}) \tag{1}$$

where B, η and μ are the magnetic field, electrical resistivity and magnetic permeability respectively, to advance the q-profile and hence the current profile in time. J_{NI} is the non-inductive current which is calculated independently in the code. For TRANSP to solve this partial differential equation numerically an initial magnetic geometry must be established.

The method adopted by the present authors was to impose the magnetic pitch angle inferred from the MSE measurements as an initial condition. Using this initialisation the current profile was evolved via field diffusion. In this way, the TRANSP run was started with enough detailed information about the current profile to enable optimised shear and even current hole scenarios to be modelled. TRANSP was then run several times using different models of the resistivity and bootstrap current but starting with the same initial conditions.

The parallel electrical resistivity in a plasma depends on the electron temperature and the local effective ion charge, Z_{eff} and in the case of neoclassical models on the trapped particle fraction. It also weakly depends on the electron density through the Coulomb logarithm. An earlier neoclassical resistivity and bootstrap current model implemented in TRANSP, developed by Hirshmann [15],[16], is valid at low inverse aspect ratio, e <<1, and arbitrary electron collisionality ν_{e*}. The multispecies code NCLASS [17], also included in TRANSP, is valid for arbitrary ε and ν_{e*}. A third model, that of Sauter [18], is a Z-effective parameterised neoclassical model which is as general as NCLASS but is more convenient to use.

Where possible the Electron Cyclotron Emission (ECE) temperature was used in the TRANSP calculation of the resistivity. A suprathermal electron population induced by lower hybrid heating, in some discharges, will corrupt the spectral shape of the ECE measured temperature. In that case

LIDAR Thomson scattering data is employed. Where the profile measurement of Z_{eff} from charge exchange was unavailable a line-integrated measurement from visible Bremsstrahlung was input. The plasma boundary, which needs to be supplied to TRANSP, was calculated by the interpretative equilibrium code EFIT [19] constrained by the external magnetics. Inside this fixed boundary the magnetic flux surface geometry is calculated using the kinetic pressure profile, including fast particle contributions, and the q-profile as constraints. TRANSP solves the poloidal magnetic diffusion equation within this fixed boundary without taking external magnetic measurements or internal MSE data into account.

The MSE diagnostic measures the polarisation angle of the Stark-split D_α emission at 25 locations. The measured angle γ_m which includes contributions from all the field components needs to be transformed to $\gamma = \frac{B_z}{B_t}$ (where B_z is the component of the poloidal magnetic field perpendicular to the major radius and B_t is the toroidal field) along the midplane to be consistent with the TRANSP pitch angle using the following approximate relation[20].

$$tan\ (\gamma_m) = tan\ \gamma\ \frac{a_0}{a_5} + \frac{a_2}{a_5} \qquad (2)$$

where $a_0 - a_5$ are geometry related factors. The error (i.e. one standard deviation) of the MSE measurement, largely due to calibration uncertainties, is about 0.2^o [13]. In general, the MSE channels #9 – #19 lying in the radial range 3.03m < R < 3.50m are reliable (the outer channels being adversely affected by the limitations of the viewing geometry of the MSE diagnostic while the inner channels often suffer from low signal strength due to beam attenuation [13]). The typical radial location of the magnetic axis is 3.0m. Where a large toroidal velocity is measured by charge exchange spectroscopy a radial electric field correction to the MSE data was carried out [20].

A typical pulse involves Lower Hybrid Current Drive (LHCD) preheating followed by neutral beam and Ion Cyclotron Resonance Heating (ICRH) heating. Since the TRANSP run must start before the neutral beam phase (due to the Monte Carlo calculation that takes place during that phase) MSE data is unavailable initially. To circumvent this, the pitch angle used at the beginning of the TRANSP run was chosen to give agreement with experiment at the time of the first MSE profile. In cases where a current hole was established in the preheating phase the restriction that a negative current cannot be maintained in this region was adhered to [21]. In fact, the TRANSP code will not allow of a region of flat pitch angle around the axis, that is the signature feature of a current hole, to be input. This was replaced by a small but finite slope in pitch angle producing the closest approximation to a current hole that the code would allow. The run was initiated using this pitch angle to calculate a q-profile. To find the q-profile at time points after the pitch angle initialisation phase the magnetic field diffusion equation was employed. The calculated pitch angle was interpolated at the MSE channel locations to facilitate comparison with the data. This analysis, carried out for over 24 JET discharges, was repeated for each model of the resistivity and bootstrap current under investigation.

The set of discharges included in the analysis covers a range of injected neutral beam powers (1 – 12MW), of ICRH input powers (up to 7MW) and include cases both with and without LHCD preheating. The beam-driven current was accurately calculated in each shot using a Monte Carlo neutral beam package [8] (the maximum fraction of beam-driven to total plasma current in the database was 33%). The effects of ICRH was modelled using a bounce-averaged Fokker-Planck code coupled with the full-wave deposition code SPRUCE [22]. MSE data was usually present during the current ramp up phase, thus allowing the measurement of a rapidly changing pitch angle and a more exacting test of the resistivity and bootstrap models. The salient features in the timing of a typical TRANSP run are illustrated in relation to the non-ohmic power input in figure 1.

3. ANALYSIS OF RESULTS

The loop voltage predicted by TRANSP is dependent on the resistivity and bootstrap model used. When this is compared to the loop voltage measured by diagnostics [23] it is clear that the NCLASS neoclassical model is more accurate than Spitzer (figure 2). The slope of the linear fit to the calculated voltage versus measured voltage data is 1.07 and 0.6 in neoclassical case and Spitzer case respectively. The loop voltage calculated by the Hirshmann neoclassical model is very similar to NCLASS. The scatter evident in the figure depends in a complicated manner on the uncertainty in the electron temperature and Z_{eff}, and since the plasma current profile is not in equilibrium, on the history of the evolution of the plasma current and the initial conditions prescribed [24]. Though the comparison of this integrated quantity finds in favour of the neoclassical models, it cannot resolve possible variations along the plasma radius.

To begin a more detailed comparison the MSE pitch angle data was employed. JET Pulse No: 53492 was preheated with LHCD and then powered with 8MW neutral beams while avoiding those Positive Ion Neutral Injectors (PINIs) which adversely affect the quality of the MSE data. ICRH energy which can also sometimes interfere with the MSE detectors is absent in this discharge. Thus, the MSE data from this discharge suffered minimal interference from these heating sources. A narrow current hole established during the LHCD phase contracts during the main heating phase. The beam-driven and bootstrap currents accounted for, at their respective maxima, just 5% and 13.5% of the total plasma current. Using the method described in the previous section, a TRANSP predicted pitch angle was calculated for each resistivity and bootstrap model. The neoclassical prediction (for each neoclassical model) was much superior to Spitzer when compared with the MSE data measured at channels #9 – #19. Furthermore, for all 14 MSE channels in the range 2.75m < R < 3.41m, the root mean squared error (rmse) of the NCLASS neoclassical prediction was less than 0.25^o (i.e comparable with the error associated with the data). The neoclassical predictions of the Hirshmann and Sauter models were similar to NCLASS. By constrast, the rmse of the Spitzer prediction, when averaged over the same set of channels was 0.47^o. The accuracy of the TRANSP prediction of the pitch angle when using a neoclassical model, in contrast to the markedly more inaccurate prediction of the Spitzer model, is illustrated for two MSE channels plotted in figure 3.

The accuracy with which the pitch angle is evolved by TRANSP is reflected in the current profile evolution. The TRANSP iota-bar and current density profile and that found by EFIT with MSE constraint is shown at the beginning, at an intermediate time, and at the end of the MSE phase in figure 4. Since TRANSP is initialised using pitch angle data, its current profile around the magnetic axis also tends towards a current hole. However, zero current around the magnetic axis cannot be admitted by the code due to numerical instabilities at overly high values of q on axis. Furthermore, since the TRANSP run starts a little before the MSE phase it follows that the pitch angle it calculates at the start of that phase (via field diffusion) will differ slightly from the measurements (as is evident in fig 4). The figure shows that the TRANSP evolved current profile is consistent with the EFIT current profile. In particular, the contraction of the current hole is well predicted by TRANSP. The oscillatory features of the latter profile not reproduced by TRANSP are artifacts of the spline model used to obtain a solution to the equilibrium equation.

From the database of pulses on which a similar analysis was carried out the conditions necessary for an accurate prediction of the pitch angle by TRANSP could be established. In the three comparisons shown in figure 5 differing behaviours of pitch angle evolution are well predicted by the code. In figure 6 plasma parameters which are pertinent to the behaviour of the pitch angle in these three pulses are plotted. In the figure 5 (a) (Pulse No: 52656 at 3.4m) the pitch angle at 5.8s rises sharply following a reduction in neutral beam and ICRH power and a consequent shifting inwards of the plasma axis (see figure 6 (a)). Conversely, in figure 5 (b) (Pulse No: 52658 at 3.36m) the magnetic axis moves outwards in the range 3.8s to 4.6s as input power is increased. At 44.8s the competing process of pitch angle increasing due to inward current diffusion begins to dominate. In figure 5 (c) (Pulse No: 53493 at 3.22m) the pitch angle data is available only intermittently due to the required neutral beam PINI being fired in so called ’blips’ (figure 5 (c)). In this case, the non-monotonicity of the pitch angle time trace is due to the ramp up and subsequent fall in the ICRH and ohmic powers. TRANSP accurately predicts the pitch angle at each ’blip’ and therefore, one might conclude, at the intervening times. The evidence of Shafranov shifting in the pitch angle in all three cases is well predicted by TRANSP when using a neoclassical model for the resistivity and bootstrap current.

As a measure of the accuracy with which the pitch angle is predicted by TRANSP, the root mean squared error $rmse_g$ was calcuated using all timepoints for each MSE channel and each pulse (and each model of resistivity and bootstrap current under consideration) in turn - see equation 3..

$$rmse_{\gamma} = \sqrt{\frac{\Sigma^{N_{time}} (\gamma_{DATA} - \gamma_{TRANSP})^2}{N_{time}}} \quad (3)$$

where γ_{DATA}, γ_{TRANSP} are the measured and predicted pitch angles respectively and N_{time} is the number of time points summed over for a particular pulse. In figure 7 the rmse at channel 3.4m, against mean neutral beam and mean ICRF power, is plotted. In both cases no clear dependency on the level of input power is evident. A similar lack of dependency prevails at MSE channels #9 – #19.

An analysis of the database showed that the mean rmse of the TRANSP prediction (when using either the Hirshmann, NCLASS or Sauter neoclassical models) of the pitch angle at MSE channels #9 – #19 (identified in section II) was approximately 0.35^o. This is within two standard deviations (2×0.2^o) of the MSE pitch angle data. The variation in this figure due to the neoclassical model used was just 3% (the Hirshmann model having the highest rmse). The mean rmse calculated at the four MSE channels in the range 3.12m-3.27m (i.e. channels #9 – #12) were above this global mean with a maximum mean rmse of 0.4^o being recorded at 3.22m. By contrast, when the Spitzer model of resistivity was used the mean rmse over all channels was 0.58^o. If the NCLASS bootstrap current is artificially included in the TRANSP run while using Spitzer resistivity the mean rmse was 0.53^o. Thus 78% of the difference in accuracy between the Spitzer and neoclassical predictions of the pitch angle is due to the resistivity component of the calculation. It is also of interest to compare the iota-bar profile of the EFIT equilibrium recontruction when constrained by MSE data with the TRANSP evolved equivalent. It should be noted that the comparison of q profile differences from distinct codes is more difficult than the corresponding iota-bar profile comparison due to the strongly non-uniform (heteroscedastic) nature of the error propagation in q: For a given uncertainty in the MSE measurement, the uncertainty in q at the location of the MSE channel scales as $\Delta q \propto q^2 \Delta\gamma$, i.e. as the square of the q value. In contrast, the uncertainty in iota-bar at a fixed location is independent of the value of iota-bar [25]. The rms difference of the TRANSP iota profile when compared to the corresponding EFIT-MSE iota-bar profile averaged over all available pulses is shown in figure 8. The rms difference is at a minimum at the plasma boundary as expected; information from the external magnetics ensure iota-bar is well defined here. As is clear in the figure, the average rms difference calculated by the neoclassical model is poor near the magnetic axis (in the radial range $2.8\text{m} < R < 3.2\text{m}$). Due to the limit on the safety factor at the magnetic axis in TRANSP, the code is unable to replicate the EFIT calculation of iota-bar in cases of extreme reversed shear in this range. The Spitzer model calculation of iota-bar in these cases is fortuitously closer to the EFIT calculation close to the magnetic axis than the neoclassical model due to the lower resistivity, and hence more slowly evolving iota-bar profile, that it calculates.

As a separate test of the predictive powers of the TRANSP code with respect to the q-profile, a comparison with MHD events was conducted. The apparent frequency of neo-classical tearing modes, measured by magnetics sensors, is n times the local bulk plasma rotation frequency (where n is the toroidal mode number of the NTM), with some small offset corresponding to the island rotation in the $\mathbf{E} \times \mathbf{B}$ frame of reference. Thus, the location of neoclassical tearing modes can be calculated using the rotation frequency profile derived from charge exchange Doppler spectroscopy [26]. This diagnostic provides rotation frequency measurements of the impurity species (carbon) which can differ substantially from that of the bulk plasma [27]. However, for the pulses under investigation here this effect on the rotation frequency was limited to 5%. This information gives a local value of the q-profile to be compared with the TRANSP calculation. This comparison was carried out on 10 pulses. In all cases the current profile was evolved using the NCLASS model. On average, the rmse of the TRANSP prediction of the position of the $q = \frac{3}{2}$ surface, when compared with the MHD inferred location of that surface, was 4cm. For example, in figure 9 the rmse of the TRANSP prediction, over the 2.5s of the existence of the NTM, is just 1.4cm. The variance in the CXS channel location, which contributes to the uncertainty in the MHD inferred location, was 3cm [28].

The consistency of the TRANSP output with polarimetric measurements of Faraday rotation was also examined. The multichannel polarimetry diagnostic at JET shares its 4 vertical and 4 lateral lines of sight with the Far Infra-Red (FIR) interferometer and measures the line-integrated product of the electron density and the parallel component of the poloidal magnetic field. The consistency test was carried out using 18 of the 24 TRANSP runs for which Faraday rotation polarimetry data was available. For the purposes of comparison, the error in the Faraday rotation angle predicted by EFIT, when constrained by MSE pitch angle data (the Faraday rotation data played no part in the equilibrium reconstruction) was also calculated. Both the TRANSP and EFIT Faraday angle calculations were normalised to agree with the data at the first time point in the EFIT run. At each polarimetry channel it was found that the TRANSP calculation of the Faraday angle was within two standard deviations (2×0.2^{o}) of the data. The percentage variation in the rmse (calculated as in eqn.3) due to the neoclassical model used in the TRANSP run, when averaged over all the pulses and polarimetry channels, was 6% (the Hirshmann model again having the highest rmse). The total mean squared error of the TRANSP and EFIT Faraday rotation predictions were calculated using the following equation

$$totalmse_{\alpha} = \sum^{N_{pulse}} \sum^{N_{channel}} \sum^{N_{time}} (\alpha_{DATA} - \alpha_{CAL})^2 \qquad (4)$$

where α_{DATA}, α_{CAL} are the measured and predicted Faraday rotation angles respectively. N_{pulse}, $N_{channel}$ and N_{time} are the number of pulses, polarimetry channels and time points to be summed over. The ratio of the TRANSP total mean squared error to that of EFIT was 1.007 when NCLASS was used to model the resistivity and bootstrap current in TRANSP but this ratio rose to 1.14 when Spitzer resistivity was used. This consistency of the TRANSP Faraday rotation calculation with both the polarimetry data and the EFIT calculation is demonstrated in figure 10.

DISCUSSION

The evolution of the pitch angle in JET as calculated by TRANSP was shown to be consistent with that measured by the motional Stark effect diagnostic when a neoclassical model of the resistivity and bootstrap current was employed. This result is in agreement with earlier investigations [9]-[11] of the resistivity model in JET. The consistency of the predicted MSE signals from TRANSP was demonstrated in a comparison of the TRANSP evolved current profile with that found by the equilibrium code EFIT when the latter was constrained by the MSE pitch angle data. This agreement was found to hold over a large range of plasma heating scenarios. In particular, TRANSP was able to follow the deterioration of a current hole in the plasma core with reasonable accuracy. The Spitzer model, as expected, was significantly less accurate than the neoclassical models in predicting the pitch angle evolution. The Hirshmann model, valid only at low inverse aspect ratio, was found to be systematically less accurate in its prediction of the MSE pitch angle and Faraday rotation angle than the NCLASS and Sauter models. No dependence on neutral beam or ICRF heating was found. The location of a specific rational surface in the TRANSP evolved q-profile was found to be consistent with MHD data. The location of neoclassical tearing modes, and hence the $q = \frac{3}{2}$ surface, was found by comparing their rotation rates with the measurements of charge exchange spectroscopy. Due to the accuracy with which TRANSP predicts the location of NTM modes, we conjecture that the effect of the modes on the magnetic field diffusion is localised. The consistency of TRANSP with other types of MHD events such as sawtooth crashes could also be examined. Finally, the evolution of the Faraday rotation angle calculated by TRANSP was found to be consistent with the polarimetry data, and also consistent with the EFIT results when the equilibrium calculation was constrained by MSE pitch angle data.

In summation, it has been shown that TRANSP, given an accurate initial pitch angle profile is accurate in its evolution of that quantity, and its derivative the current profile, thereafter. Potentially, this should enable the current profile to be calculated with (modest) uncertainties typified by the results presented here even in the absence of MSE data in the following situations: (i) After a period of availablity early in the discharge there is no further usable MSE data due to the deployment of an unfavourable combination of NBI sources, etc. (ii) Assuming a standard pre-heating scenario with a reproducible early current profile evolution as verified from discharges with MSE data, it becomes feasible to use TRANSP to evolve the current profile for discharges with the same early phase (thus providing a reliable initial condition) where no MSE data are available. Extending this work to include those pulses with LHCD during the main heating phase would markedly increase the range of pulses that could be modeled using the technique presented here and work is in progress to achieve this.

ACKNOWLEDGEMENTS

The authors would like to thank D. McCune for discussions on the resistivity and bootstrap models in TRANSP, J. Conboy for software support of the code, K-D Zastrow for analysis of the charge exchange data and D. Howell, S. Pinches and D. Testa for assistance with MHD data. This work was performed under the European Fusion Development Agreement and was supported by the EURATOM Mobility programme. The work carried out by the UKAEA personnel was jointly funded by the United Kingdom Engineering and Physical Sciences Research Council and by EURATOM.

REFERENCES

[1]. R.V. Budny et al., Phys. of Plas. **7** 5038 (2000)

[2]. L. Spitzer and R. Harm, Phys. Rev. **89**, 977 (1953)

[3]. M.C. Zarnstorff et al Phys. Fluids B **2** 1852 (1990)

[4]. M. Kikuchi et al Nucl. Fusion **30** 343 (1990)

[5]. D.J. Campbell et al Nucl. Fusion **28** 981 (1988)

[6]. S.H. Batha et al Phys. Plasmas **4**(10) 3614 (1997)

[7]. E. Joffrin et al Plasma Phys. Control. Fusion **42** 1227 (2000)

[8]. R.J. Goldston, D.C. McCune et al, J. Comp. Phys, **43**, 61 (1981)

[9]. D.V. Bartlett et al Nucl. Fusion **28** 73 (1988)

[10]. D.J. Ward Plasma Phys. Control. Fusion **36** 673 (1994)

[11]. T.J.J. Tala et al Plasma Phys. Control. Fusion **44** 1181 (2002)

[12]. C.B. Forest et al Phys. Rev. Lett. **73** 2444 (1994)

[13]. N.C. Hawkes et al Rev. Sci. Inst. **70**(1) 894 (1999)

[14]. N.C. Hawkes et al Phys, Rev. Lett.**87**(11) art. no. 115001 (2001)

[15]. S.P. Hirshman, R. J. Hawryluk, B. Birge, Nucl. Fusion **17**, 611 (1977)

[16]. S.P. Hirshman, Phys. Fluids, **21** 1295 (1978)

[17]. W.A. Houlberg, K. C. Shaing, S. P. Hirshman and M.C Zarnstorff, Phys. Plasmas **4** 3230 (1997)

[18]. O. Sauter, C. Angioni and Y. R. Lin-Liu, Phys. Plasmas **6**(7) 2834 (1999)

[19]. L. Lao et al, Nucl. Fusion **29**, 563 (1985)

[20]. N.C. Hawkes et al Plasma Phys. Control. Fusion **44** 1 (2002)

[21]. Huysmans GTA, Hender TC, Hawkes NC, et al Phys. Rev. Lett. **87**(24): art no 245002 (2001)

[22]. M. Evrard et al, in AIP Conference Proceedings 355, Radio-Frequency Power in Plasmas, 11th topical conference, Palm Springs (1995) p.235

[23]. J.P. Christiansen, J. Comp. Phys **73**, 85 (1987)

[24]. D.C. Mc Cune, private communication

[25]. P.J. McCarthy, M. Foley et al,Proc 30th Eur. Conf. on Contr. Fusion Plas. Phys. 26B (EPS Montreux 2002)

[26]. R.J. Buttery et al, Nucl. Fusion **43** 69 (2003)

[27]. D. Testa et al, Phys. Plasmas **9** 243 (2002)

[28]. K.D. Zastrow, private communication

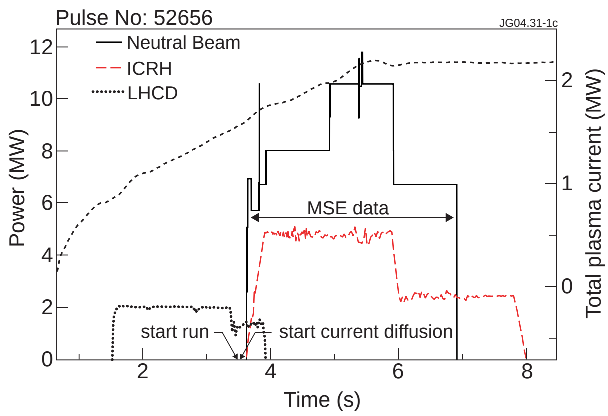

Figure 1: Illustration for a typical input power scenario of the time sequence for the start of the TRANSP run, the start of current diffusion in the code, the availability of MSE data and the non-ohmic power input. The evolution of total plasma current is also shown.

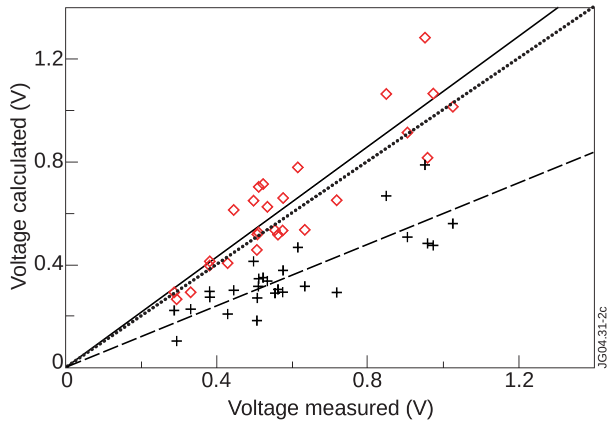

Figure 2: Comparison of the loop voltage calculated by TRANSP with that measured. Predictions were made using NCLASS (diamonds) and Spitzer (crosses) resistivity models. As well as the y = x line (dotted), the linear fits (of form y = slope ∗ x) to the NCLASS (bold line) and Spitzer (dash) predictions are included. An error bar of 10% applies to the measured voltage.

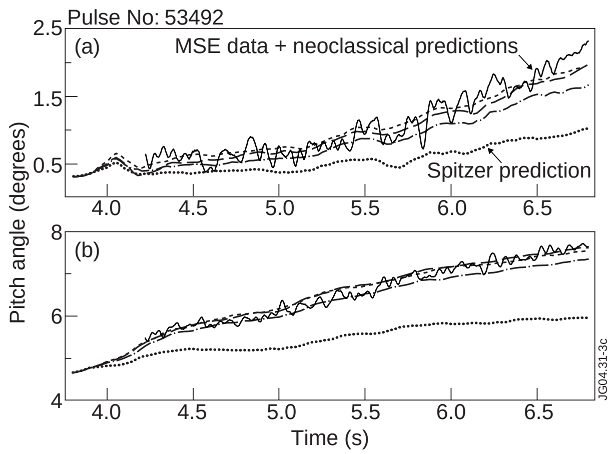

Figure 3: Comparison of the pitch angle calculated by TRANSP with that measured (full line) by MSE at channel (a)3.07m and (b)3.36m. Predictions were made using NCLASS (dashes), Sauter (dash-dot-dot), Hirshmann (dash-dot) and Spitzer (dots) resistivity models. The raw MSE data was averaged over ±15ms.

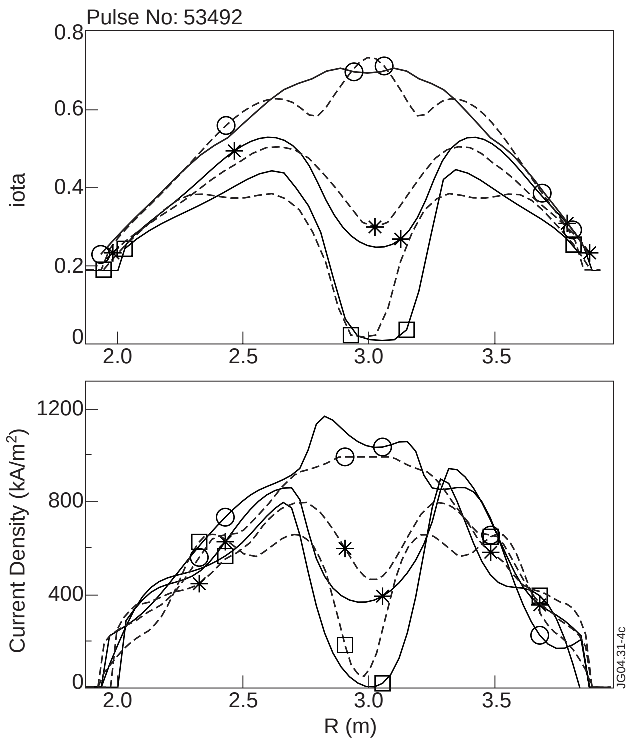

Figure 4: Iota-bar and current profile at the start(squares), at an intermediate time (stars) and at the end(circles) of MSE data calculated by EFIT+MSE (solid line) and TRANSP (dots) (Pulse No: 53492 at times 44.1s, 45.0s and 46.7s)

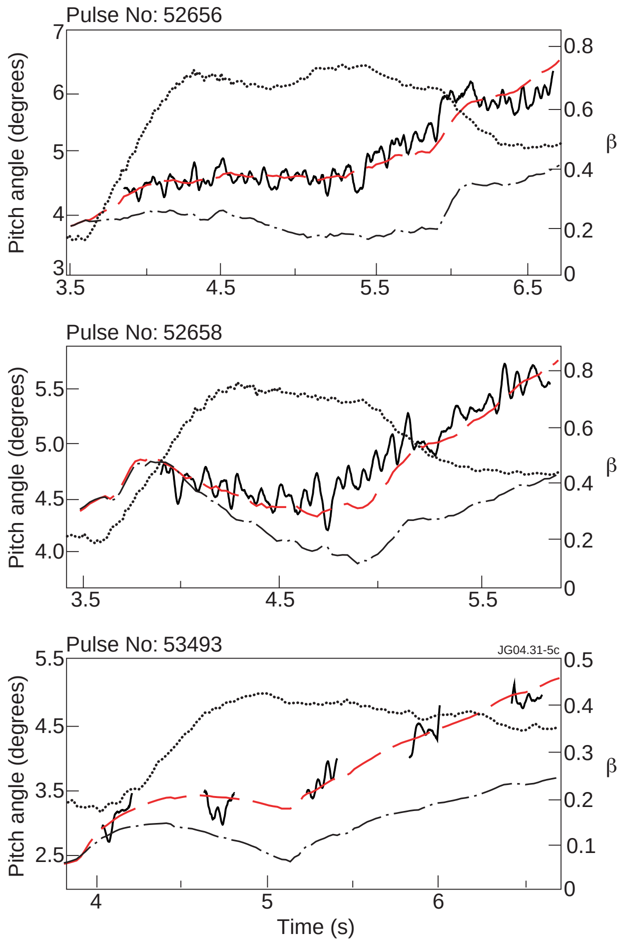

Figure 5: Comparison of the pitch angle calculated by TRANSP with that measured (full line) by MSE at one channel from three pulses: (a) 52656 at 3.4m (b) 52658 at 3.36m and (c) 53493 at 3.22m. Predictions were made using NCLASS (dashes) and Spitzer (dash-dots) resistivity models. Beta poloidal (dot) is also included.

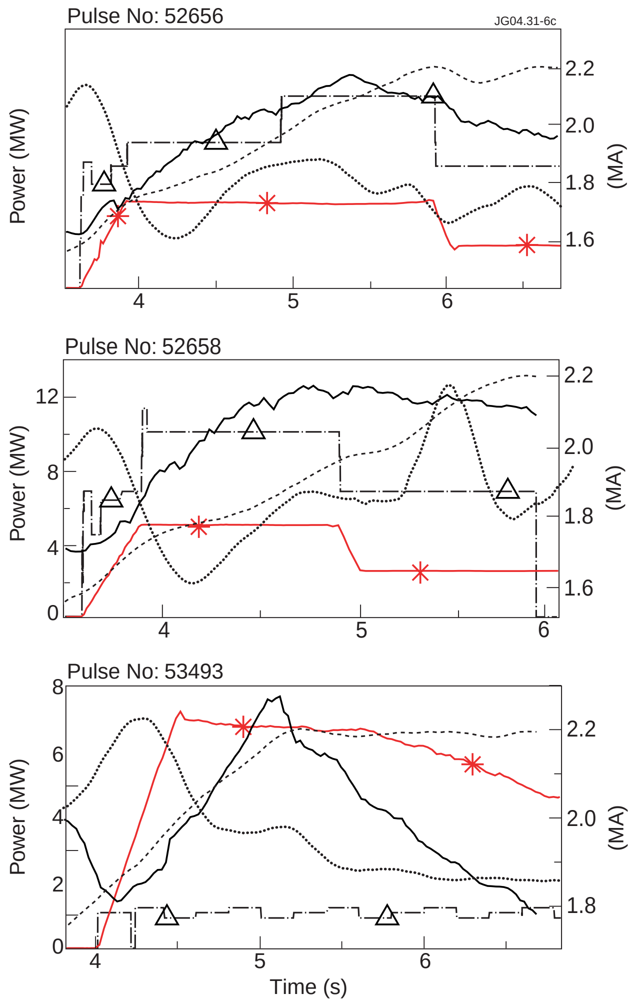

Figure 6: Total plasma current (dash), neutral beam (triangles) and ICRH (stars) power corresponding to the three pulses in fig.5. The magnetic axis location (bold) and loop voltage (dots) are also shown without scale. The maximum variation in the magnetic axis location in the three plots is (a) 20cm, (b) 13cm and (c)6cm while that of the loop voltage in all cases is approx. 0.6V.

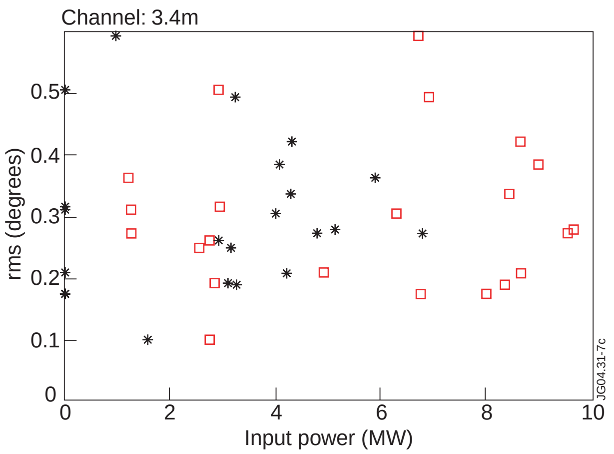

Figure 7: Root mean squared error of pitch angle prediction against neutral beam power (squares) and ICRH power (stars) for each shot in the database at 3.4m

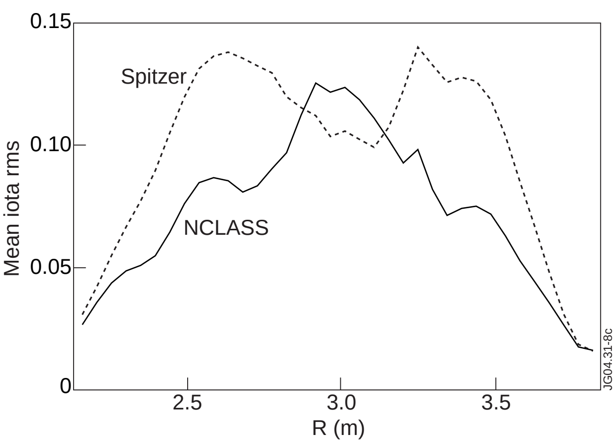

Figure 8: Profile (database average) of root mean square difference between TRANSP and EFIT+MSE iota-bar profiles calculated using the NCLASS (full) and Spitzer (dashes) restivity models.

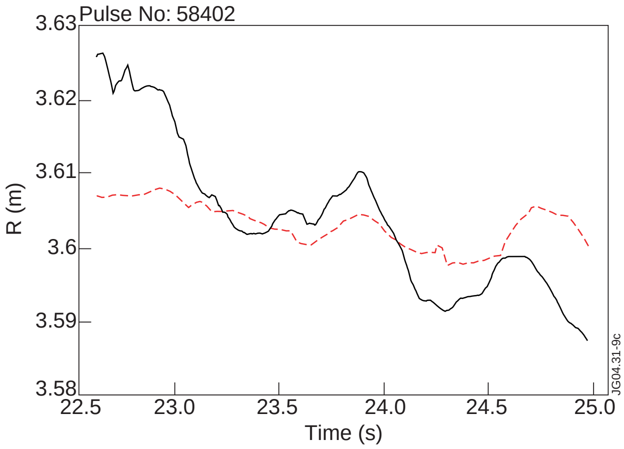

Figure 9: The location of the TRANSP q=3/2 surface using neoclassical resistivity (dashes) compared to that inferred by MHD (solid).

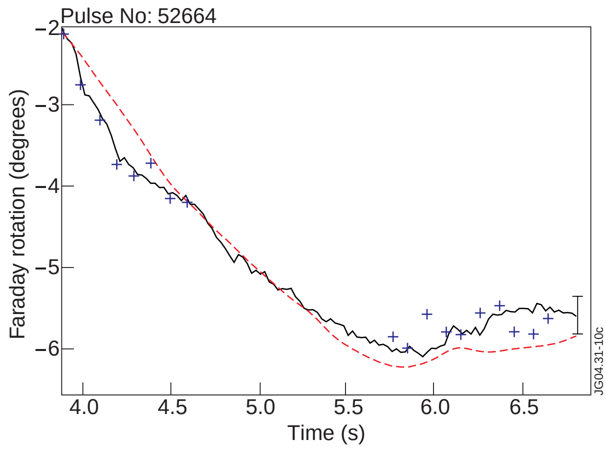

Figure 10: Comparison of the Faraday rotation angle calculated by TRANSP (dotted line) and EFIT+MSE (symbols) with that measured by polarimetry (solid) for Pulse No: 52664 at Faraday channel no.2. One standard deviation in the polarimetry data is indicated by the error bar. The hiatus in the EFIT prediction in the interval 44.6 – 45.8s is due to an absence of reliable MSE data.